# Supplementary information

# Immobilisation of β-galactosidase within lipid sponge phase: structure, stability and kinetics characterisation

*Jennifer Gilbert[a,b], Maria Valldeperas[a,c], Surender K. Dhayal[d], Justas Barauskas[e], Cedric Dicko[f] and Tommy Nylander[a,c,g]*

[a] Physical Chemistry, Department of Chemistry, Lund University, P.O. Box 124, SE-22100 Lund, Sweden

[b] Department of Chemistry, University of Southampton, University Road, Southampton SO17 1BJ, United Kingdom.

[c] NanoLund, Lund University, P.O. Box 118, SE-22100 Lund, Sweden.

[d] Biotechnology, Chr. Hansen Holding A/S, Boege Alle 10-12, 2970 Hoersholm, Denmark

[e] Camurus AB, Ideon Science Park, Gamma Building, Sölvegatan 41, SE-22379 Lund, Sweden.

[f] Pure and Applied Biochemistry, Department of Chemistry, Lund University, P.O. Box 124, SE-22100 Lund, Sweden

[g] LINXS - Lund Institute of Advanced Neutron and X-ray Science, Scheelevägen 19 22370 LUND, SWEDEN

## Sample preparation

*Dialysis of β-galactosidase – 10mM phosphate buffer*

Dialysis of Ha-lactase was performed following a similar procedure to the one described in the main paper. In this case, 100-150 mL of Ha-lactase was added to the dialysis bag (around 50 cm). The dialysis was done against 10 mM sodium phosphate buffer and 2mM $NaN_3$ at pH7 over 4 days at 4°C. The dialysis membrane was placed in a cylinder of 2 L that was filled with buffer. The conductivity of the buffer was monitored until it was the same as the original buffer. The dialysed β-galactosidase was concentrated and adjusted using the 10mM phosphate buffer as described in the main paper.

## Estimating Water Channel Radius:

This section contains a summary of the method devised by Valldeperas et al.[1] to calculate the water channel radius of the sponge phase using the water channel radius of the cubic phase immediately preceding it along the dilution line in the phase diagram.

The monolayer thickness, l, was determined for the cubic phase (modelled as an infinite periodic minimal surface (IPMS)) using experimentally determined lattice parameters, $a_{cubic}$.

The molecular cross sectional area, A, at a distance ξ from the IPMS and integrated over the monolayers within the unit cell can be modelled by the following equation:[2,3]

$$A(\xi) = A_0 a_{cubic} + 2\pi\chi\xi^2$$

where $A_0$ is the ratio of the IPMS area to (unit cell volume)$^{2/3}$ and χ is the Euler-Poincare characteristics, both of which are constant defined by the cubic space group.

Using the fact that $A(\xi) \to 0$ at the centre of the water channel and $\xi = l + r_w$, the above equation can be rewritten as:[3]

$$r_{w-cubic} = -\sqrt{\frac{A_0}{2\pi\chi}}a_{cubic} - l$$

The d spacing of the cubic phase and sponge phase can be determined from the first peak of small angle x-ray scattering (SAXS) data:

$$d = \frac{2\pi}{q}$$

The water channel radius of the sponge phase can then be estimated by multiplying the water channel radius of the cubic phase by the ratio of the d-spacing of the sponge and cubic phase immediately preceding it:

$$r_{w,\ L3} = \frac{d_{L3}}{d_{cubic}}\, r_{w,\ cubic}$$

For this paper, the following values from Valldeperas et al.[1] were used to calculate the water channel radius of the sponge phase: $r_{w,Q}$ = 42.13 Å, $d_Q$ = 120.97 Å.

## Size exclusion chromatography – Data Analysis

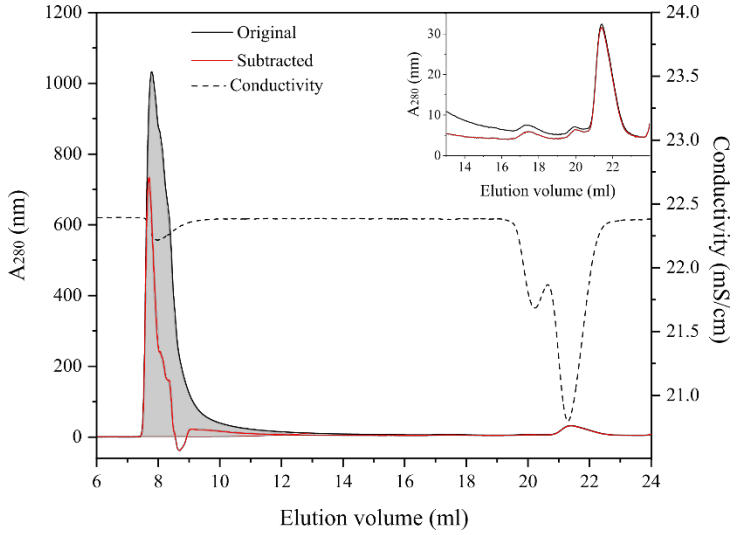


**Figure S1.** Absorbance and conductivity as function of elution volume of Encapsulated β-galactosidase - Day 1. Black line shows the raw data, while the red line is the curve obtained after subtracting the contribution of the corresponding elution curve from the enzyme free 40mg/ml $L_3$-NP dispersion. Grey area shows the AUC of the nanoparticle peak given in Table 5. The embedded plot displays a magnification of the 15-24ml region.

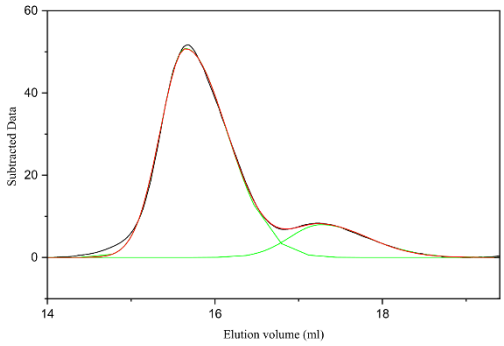


**Figure S2.** SEC data analysis of two enzyme peaks for 3 mg/ml dialysed β-galactosidase after baseline correction. All the peaks were fitted with a bigaussian function (green line) and then each of them were integrated to obtain the area.

## Effect of β-galactosidase on $L_3$ Structure – 10 mM phosphate buffer

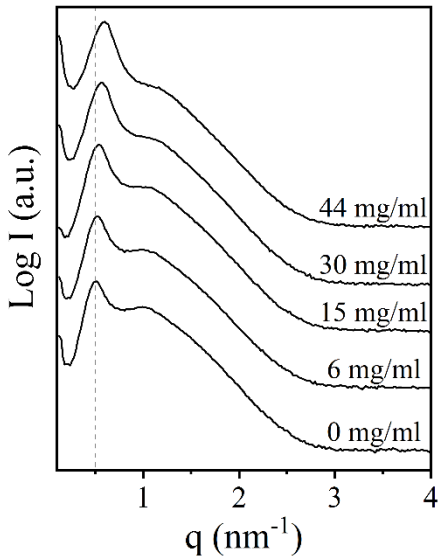


**Figure S3.** SAXS data for 28/42/30 DGMO/GMO-50/P80 system with different concentrations β-galactosidase in 10 mM sodium phosphate buffer. Final β-galactosidase concentration is indicated on the plot. All samples were isotopic under cross polarized light and did not present water excess, except at the highest protein concentration studied. It should be noted that, for comparison with the SAXS data presented in the paper, this data was collected for a wider range of β-galactosidase concentrations.

## Cryo-TEM Images of $L_3$NPs containing β-galactosidase

The structure and morphology of the $L_3$NPs containing β-galactosidase was imaged using cryo-TEM, as described previously [4]. Nanoparticles with the characteristic disordered structure of the $L_3$ phase were indeed observed even with included β-galactosidase.

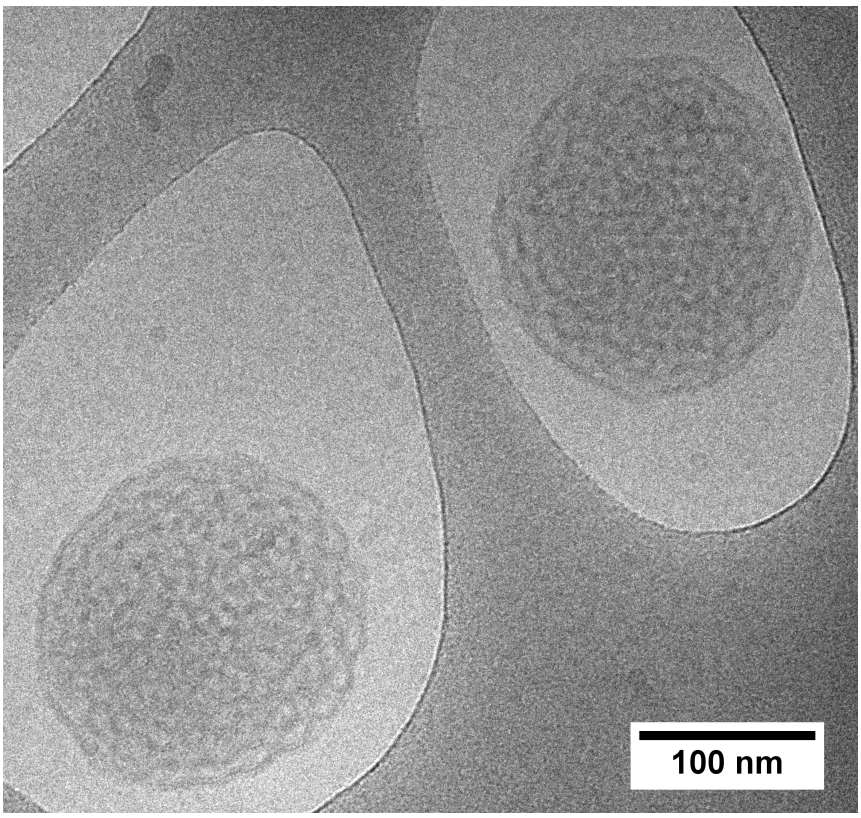


**Figure S4**: Cryo-TEM images of $L_3$-NPs containing β-galactosidase.

## Dynamic light scattering of β-galactosidase

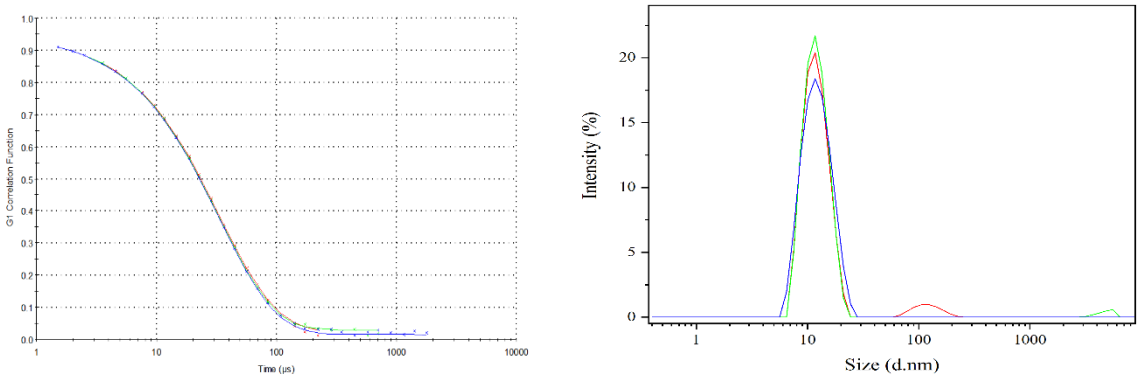


**Figure S5.** Determination of the β-galactosidase hydrodynamic diameter assuming a spherical shape (performed in triplicate). Left: Correlation function of the data (crosses) and the corresponding fits (line) used to determine the size. Right: Size distribution profile obtained from the fits. The sample was prepared with 50mM phosphate buffer and 13.8 mg/ml β-galactosidase.

## Dynamic light scattering of $L_3$NPs with and without β-galactosidase

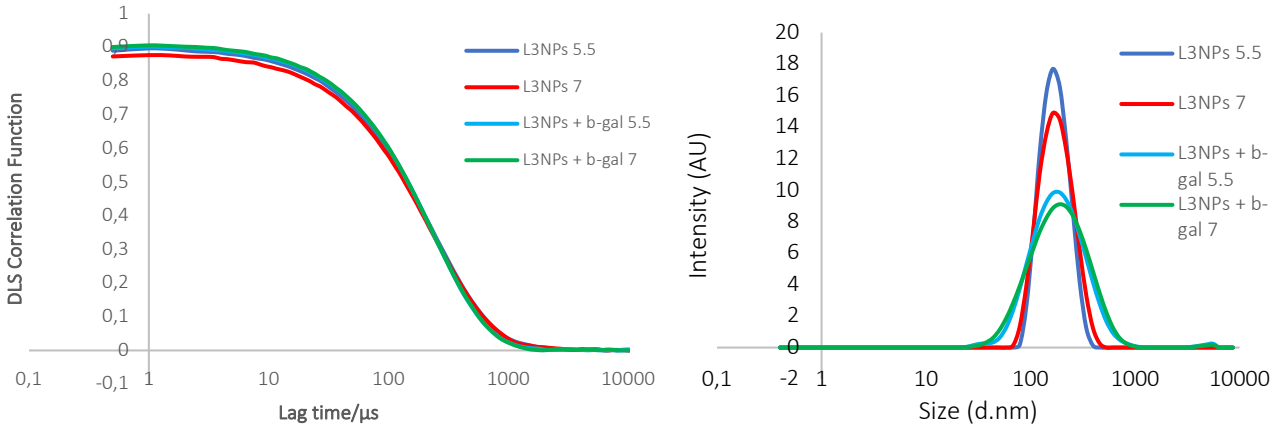


**Figure S6.** Determination of the hydrodynamic diameters of LNPs with and without β-galactosidase at different pHs. Left: Correlation functions of the data used to determine the size. Right: Size distribution profiles obtained from the fits. The samples were prepared with 5mg/ml LNPs with and without β-galactosidase and 10mM acetate buffer (pH5.5) or 10mM phosphate buffer (pH7).

**Size exclusion chromatography "calibration curve"**

The calibration curve was performed using the elution volumes of two reference proteins (Ferritin of 440 kDa and Aprotinin of 6.5 kDa) and assuming that the first peak in Thermolase [5,6] formulation is the Aspartic protease monomer of 34 kDa. It should be noted that to obtain more accurate results, more references with known molecular weight should be analysed.

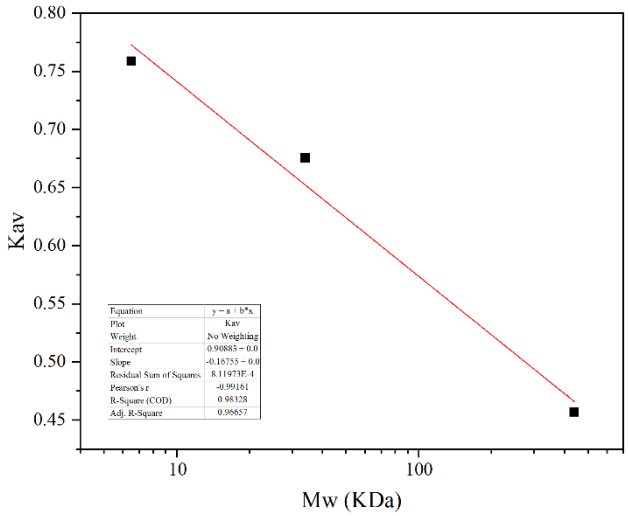


**Figure S7.** Preliminary calibration curve used to determine the molecular weight of the main β-galactosidase peak.

## Calibration curves:

*Determining molar extinction coefficient from Beer-Lambert Law*

Beer-Lambert Law states that:[7]

$$A = \varepsilon c l$$

Where A = Absorbance, C = Concentration ($moldm^{-3}$), l = Path length (cm), ε = Molar extinction coefficient ($M^{-1}cm^{-1}$).

If A is plotted against C, from the general equation of a 1st order polynomial y = mx + c, the gradient, m, is εl. For these experiments, cuvettes with a path length of 1cm were used, therefore m = ε.

*Dialysed β-galactosidase (DL)*

10x to 100x dilutions of stock of dialysed β-galactosidase of known concentration were made using 50 mM sodium phosphate buffer + 1mM $MgCl_2.6H_2O$ (pH 7.26). The absorbance at 280 nm was measured using a Varian Cary 300 Bio UV-Visible Spectrophotometer in Scan mode (250 nm-800 nm) using 50 mM sodium phosphate buffer + 1mM $MgCl_2.6H_2O$ (pH 7.26) as a baseline. The absorbance at 280 nm was plotted against concentration of dialysed β-galactosidase, fit with a first order polynomial and the gradient used to calculate the molar extinction coefficient as 160400 $M^{-1}cm^{-1}$.

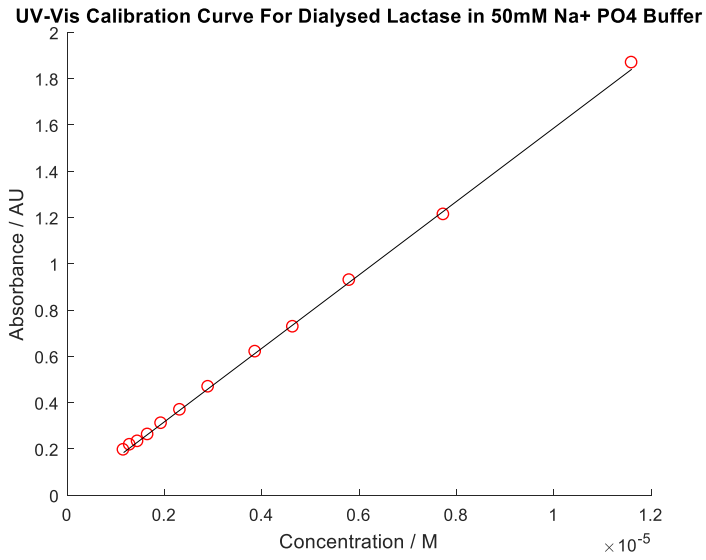


**Figure S8.** Calibration curve at 280 nm for DL in 50 mM sodium phosphate buffer + 1 mM $MgCl_2$.

*O-nitrophenol (ONP)*

10x to 100x dilutions of stock of 5 mM ONP in 52.5 mM sodium phosphate buffer + 1.05 mM $MgCl_2.6H_2O$ (pH 7.26) were made using 52.5 mM sodium phosphate buffer + 1.05 mM $MgCl_2.6H_2O$ (pH 7.26). The absorbance at 420 nm was measured using a Varian Cary 300 Bio UV-Visible Spectrophotometer in Scan mode (250 nm-800 nm) using 52.5 mM sodium phosphate buffer + 1.05 mM $MgCl_2.6H_2O$ (pH 7.26) as a baseline. The absorbance at 420 nm was plotted against concentration of ONP, fit with a first order polynomial and the gradient used to calculate the molar extinction coefficient as $2388 M^{-1}cm^{-1}$.

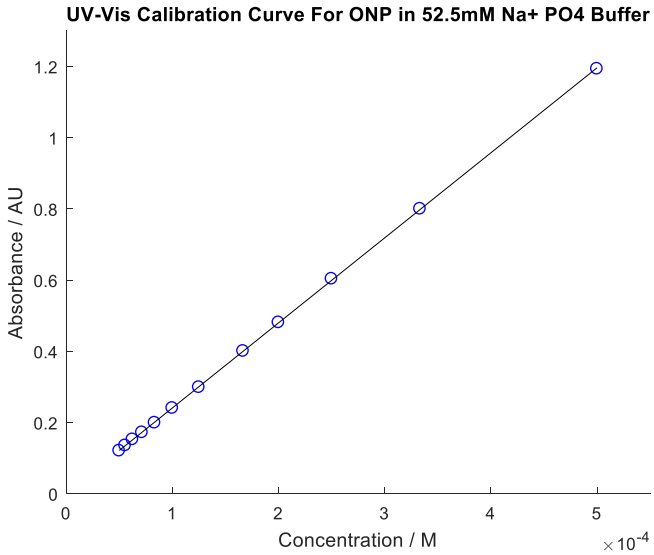


**Figure S9.** Calibration curve at 420 nm for ONP in 52.5 mM sodium phosphate buffer + 1.05 mM $MgCl_2$.

## Determining the effect of dialysis and concentration on the structure of β-galactosidase:

*Determining the enzyme activity using ONPG*

An activity test was carried out as detailed in the Methods and Materials section using HL, DL and concentrated dialysed β-galactosidase (CDL). The results were processed as detailed in the main paper, with the exception that the activity was not normalised to HL activity. The results are shown in Table S1 and indicate that 96% activity is retained for CDL and 83% activity is retained for DL.

**Table S1.** Activity of HL, DL and CDL determined using ONPG.

| Sample | Activity / NLU/g |
|---|---|
| HL | 215.2 |
| DL | 178.7 |
| CDL | 206.9 |

*Circular Dichroism (CD) Spectropolarimetry Data*

Stock solutions of HL, DL and CDL were diluted 100x with 50 mM sodium phosphate buffer + 1 mM $MgCl_2.6H_2O$ (pH 7.26). This dilution was then diluted a further 10x with water. CD spectra of these final dilutions were acquired using a Jasco J-715 Spectropolarimeter using 1mM quartz cuvettes. Data was collected in the wavelength range 185 nm – 300 nm at 25 °C and averaged over 8 measurements. The data was processed using the online CAPITO tool using buffer subtraction and smoothing with a Savitzky-Golay filter.[8] All relevant structural data required for processing, including the number and sequence of amino acids, was taken from Pereira-Rodríguez et al.[9] The data was plotted (Figure S7) and used to calculate the estimated proportions of secondary structures within the protein using the CAPITO tool (Table S2).

Generally, for all the β-galactosidase samples (HL, DL, CDL), the β-sheet proportion of the structure is approximately constant, however there is a significant decrease in the helix proportion of the structure after dialysis (DL), which remains low after concentration (CDL). Taking into account the activity data for these samples, it does not seem that the helical structures within β-galactosidase are key components for enzyme activity. It is possible, however, that this change in secondary structure affects the way in which the β-galactosidase is localised within the sponge phase.

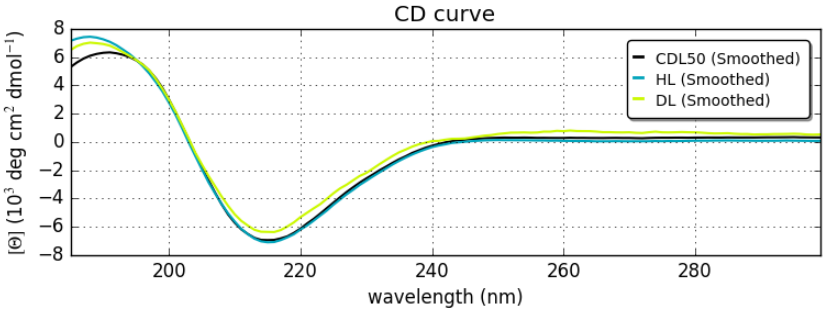


**Figure S10.** CD data for HL, DL and CL processed using the online CAPITO tool.[5]

**Table S2:** Summary of structural information from CAPITO.

| Sample | % Helices | % β-sheet |
|---|---|---|
| HL | 17 | 48 |
| DL | 5 | 47 |
| CDL | 4 | 46 |

## References


1 M. Valldeperas, M. Wiśniewska, M. Ram-On, E. Kesselman, D. Danino, T. Nylander and J. Barauskas, *Langmuir*, 2016, **32**, 8650–8659.

2 D. M. Anderson, S. M. Gruner and S. Leibler, *Proc. Natl. Acad. Sci. U. S. A.*, 1988, **85**, 5364–5368.

3 J. Briggs, H. Chung and M. Caffrey, *J. Phys. II*, 1996, **6**, 723–751.

4 M. Valldeperas, A. P. Dabkowska, G. K. Pálsson, S. Rogers, N. Mahmoudi, A. Carnerup, J. Barauskas and T. Nylander, *Soft Matter*, 2019, **15**, 2178–2189.

5 THERMOLASE®,https://www.chr-hansen.com/en/food-cultures-and-enzymes/cheese/cards/product-cards/thermolase (accessed on 18 December 2018).

6 M. Valldeperas, M. Talaikis, S. K. Dhayald, M. Veličkae, J. Barauskas, G. Niaura and T. Nylander, *Biophys. J.,* 2019, **117,** 829-843.

7 D. F. Swinehart, *J. Chem. Educ.*, 1962, **39**, 333.

8 C. Wiedemann, P. Bellstedt and M. Görlach, *Bioinformatics*, 2013, **29**, 1750–1757.

9 Á. Pereira-Rodríguez, R. Fernández-Leiro, M. I. González-Siso, M. E. Cerdán, M. Becerra and J. Sanz-Aparicio, *J. Struct. Biol.*, 2012, **177**, 392–401.